Preliminary Design Estimation of the V/STOL Airplane Performance

Murat Bronz, Antoine Drouin

Preliminary Design Estimation of the V/STOL Airplane Performance

Murat Bronz*, Antoine Drouin‡
ENAC; UAV Lab ; 7 avenue Edouard-Belin, F-31055 Toulouse, France
Université de Toulouse ; ENAC; F-31077 Toulouse, France

Abstract

A preliminary study on estimating aerodynamic forces of a Vertical/Short Takeoff and Landing (V/STOL) mini Unmanned Air Vehicle (UAV) configuration with Distributed Electric Propulsion (DEP) system is presented. The main objective is to offer the next generation fixed wing mini UAV aircraft configuration with high-speed cruise flight and vertical take-off capabilities. The proposed concept uses four electric motors and propellers combination located on the leading edge of the wing. The described method uses semi-empirical formulations in order to estimate the forces and moments generated by the wing immersed in its distributed propeller slipstreams. Actuator disk theory is used for the propeller slipstream, where the thrust is assumed to be known for the calculations. Upwash of the fuselage and each propeller slipstream are taken into account for the wing and propeller inflow angle calculations. The resulting method, which is written as a program, serves as a conceptual design program for this type of configuration. Additionally, the program will be used for generating data for flight dynamics simulations. A candidate design is also presented, which is being manufactured for the on-going developments and tests.

1 Introduction

In the past decade performance of small electric rotorcraft have improved vastly whereas performances of fixed wing vehicles have improved much less. For a number of applications that focus on high velocity and long range, fixed wing vehicles remain the best choice. The main limiting factor for the fixed wing configuration is the compromise between low and high velocity regimes. If the vehicle is optimized for low velocity (low wing loading, high static thrust), takeoff and landing will be easy but performances in endurance, range and high speed flight capability will be degraded because of unnecessary wing surface and low propeller efficiency during high speed flight. On the contrary, if the vehicle is optimized for speed and range (high wing loading, high pitch propellers), landing and takeoff become problematic, requiring the use of long runways and/or external devices like bungees or landing net. On large scale vehicles (often powered by combustion or jet engine), the problem is solved by the use of variable geometry (flaps, slats, variable pitch propeller). Those solution are incompatible with small scale UAVs in terms of added weight and complexity.

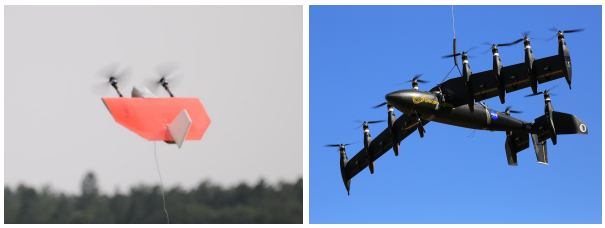

Fig. 1: Tilt-Body micro air vehicle *MAVION* and a small demonstrator of NASA's *GL-10*

Electric propulsion offers new possibilities compared to traditional jet or combustion engine solutions. NASA has started investigating DEP [1, 2]and highlighted a significant increase of efficiency for the cruise. GL-10, shown in Figure 1 is being tested for vertical take-off capability with tilting its wing and an efficient cruise by adapting its multiple propellers that are located on the leading edge of the wing. On the small scale, ISAE's *MAVION*, also shown in Figure 1, is a good example of a hand-release vertical take-off and afterwards transition to cruise flight concept. However its relatively low-pitched propellers, required to fly stationary, and low aspect ratio wings, mainly a result of size restriction, limits its high speed capability as well as endurance and range performance.

Furthermore, recent progress on automatic control[3, 4] allows the use of unstable aerodynamic configurations, as well as the use of electric motor for fast dynamic control (as is done on quadrotors). We believe that the combination of DEP and active control can be used to design the new generation of fixed wing vehicles offering superior endurance and range performance for wide velocity envelope. This includes a *hand-release* take-off, transitioning to level cruise flight while maintaining equilibrium through every attitude in between. Efficient high speed performances will be achieved

*murat.bronz@enac.fr
‡drouin@recherche.enac.fr

Fig. 2: Transitioning from four propeller stationary vertical take-off to two propeller high speed cruise phase.

thanks to folding down the big low-pitched propellers and use the high-pitched propellers only, as depicted on Figure 2.

1.1 Background

The propeller wing interaction has been vastly studied for V/STOL vehicles. The problem is highly complex to solve without simplifications. Empirical formulas have been developed by Jameson [5] in order to avoid massive calculations with the aim of estimating the generated lift and drag force. He relied on theoretical results for a rectangular wing in a constant and continuous rectangular jet slipstream. However, he has further improved the method by taking into account individual rectangular or circular slipstreams. De Young [6] has developed a method for inclined propeller forces. Jameson's simplified formulas are verified by several experimental studies [7, 8] with good agreement. It should be noted that only the lift and drag forces were calculated in those studies, and the drag force included only the induced drag.

1.2 Present Work

This study focuses on a smaller scale vehicle, where the low Reynolds number flow regime plays a major role on the performances of the vehicle. We want to estimate the performances of the vehicle both in terms of aerodynamics and flight dynamics, so the stability is also taken into account in detail. Once the complete procedure finished, it will be possible to evaluate multiple design variables (span, surface, battery capacity,etc...) changes and their effect on the final performance of the aircraft for a given mission profile. As we concentrate on high speed computation with this simplified method, it will be possible to sweep through a wide range of candidate aircrafts individually and define the best performing one.

2 Aerodynamic Model for Propeller Wing Combination

The procedure developed by Jameson[5] in order to estimate the aerodynamic forces and moments of a propeller wing combination will be described in detail for the consistency of this study. An arbitrary number of propeller slipstreams is defined, with individual thrust, actuator disk area, position and orientation. In this study, the fixation between the propeller actuator axis and the wing is fixed, however the presented model can be applied for tilting actuators as well. The method is mainly based on momentum theory, so that the swirl effects of the propeller slipstream are not modeled. DeYoung's method is used to estimate the inclined propeller thrust. Some of these previous methods are reformulated here in order to clarify the estimation procedure.

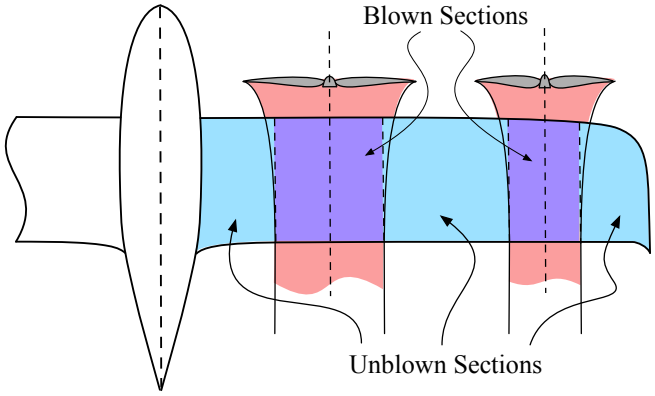

Fig. 3: Showing the creation of wing sections according to the fully developed propeller slipstream width. Note that for each thrust value the sections will dynamically be changed in order to take into account the contraction.

2.1 Propeller Forces

The propeller forces are modeled according to actuator disk theory, for a given propeller thrust T, the ratio μ, between the free stream V_∞ and propeller jet slipstream V_j, for a given actuator area of S_p is given by

$$\mu = \frac{V_\infty}{V_j} = \sqrt{1 - \frac{T}{0.5\rho V_j^2 S_p}} \tag{1}$$

Each individual slipstream is taken as circular form, and their contraction can be estimated with

$$b_{pc} = b_p \sqrt{\frac{1+\mu}{2}} \tag{2}$$

where, b_p is the propeller disk diameter or width, and b_{pc} is the fully developed contracted slipstream diameter or width. Once the contracted slipstream diameter is calculated, the wing can be separated into sections, as shown in Figure 3, that are inside the propeller slipstream or outside. Note that the propeller slipstream is taken as fully developed for simplification reasons.

2.2 Propeller Downwash

Inclined propellers will deflect the free stream, which will change the angle of attack of the wing inside this slipstream. This downwash ϵ can be determined according to the inflow angle of the propeller α_j.

$$\epsilon = E\alpha_j \tag{3}$$

according to Ribner[9] and De Young[6] where,

$$E = \frac{E_\infty}{2}\left[\frac{\frac{2x}{b_p}+e+\sqrt{1+\left(\frac{2x}{b_p}+e\right)^2}}{\frac{2x}{h_p}+e}\right] \tag{4}$$

$$E_\infty = \frac{1-\mu}{1+\mu^2}+\frac{\mu}{4}\frac{2+\mu+\mu^2}{1+\mu^2}\frac{4.25\sigma}{1+2\sigma}\sin(\beta+8) \tag{5}$$

$$e = \frac{E_\infty}{2\sqrt{1-E_\infty}} \tag{6}$$

As the slipstream form is taken circular, the propeller height h_p is equal to the propeller width b_p, and x represents the distance between actuator disk and the wing leading edge. Solidity of the propeller σ can be calculated by $\frac{4N_b}{3\pi}\frac{\bar{c}_b}{b_p}$, where $\bar{c}_b$ is the average blade chord which can be estimated by (17).

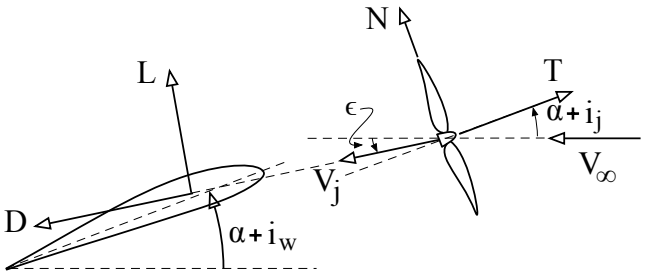

Fig. 4: Shows the wing incidence angle i_w, jet incidence angle i_j, angle of attack of the fuselage α with the resultant lift L, drag D, thrust T and the propeller normal force N, propeller downwash ϵ, jet slipstream V_j.

2.3 Actuator Inflow Angle Change due to Wing, Fuselage and Other Propeller Jets Upwash

Each actuator will be influenced by the fuselage, wing, and the other propeller jets. Taking these into effect, the inflow angle for each jet will be the sum of

$$\alpha_j = \alpha + i_j + U_w(\alpha+i_w) + U_f\alpha + \sum_{otherjets} U_{o_j}\epsilon \tag{7}$$

where, U_w is the upwash due to wing,

$$U_w = \frac{2\mu AR}{9(AR+10)}\left[\frac{1}{x_{L.75/\bar{c}}+0.1}+\frac{1}{x_{R.75/\bar{c}}+0.1}\right] \tag{8}$$

U_f is the upwash due to fuselage which is treated as an infinite falling cylinder,

$$U_f = \frac{\mu}{8}\left[\left(\frac{D_{fus}}{y_{L.75}}\right)^2+\left(\frac{D_{fus}}{y_{R.75}}\right)^2\right] \tag{9}$$

and U_{0_j} is the upwash due to the other propeller slipstreams treated as semi-infinite falling cylinders.

$$U_{0j} = \frac{\mu}{16}\left[\left(\frac{b_j}{\Delta y_{L.75}}\right)^2+\left(\frac{b_j}{\Delta y_{R.75}}\right)^2\right] \tag{10}$$

$x_{L.75/\bar{c}}$ and $x_{R.75/\bar{c}}$ are the distance between wing leading edge and propeller blade right and left 0.75 radius location. $y_{L.75}$ and $y_{R.75}$ are the distance from fuselage axis to the propeller blade right and left 0.75 radius location. $\Delta y_{L.75}$ is the lateral distance from one propeller axis to the other propeller's left blade 0.75 radius location, and $\Delta y_{R.75}$ is the right blade 0.75 radius location.

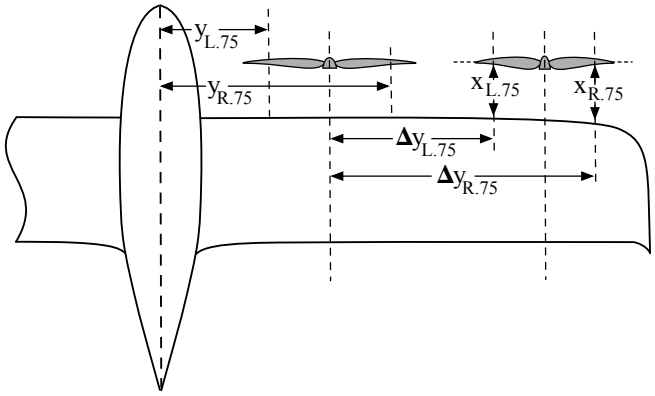

Fig. 5: Showing the incidence angles, angle of attack of the wing and actuator with the resultant lift, drag, thrust and the propeller normal force.

For each propeller slipstream , α_j can be written as

$$\begin{aligned}
\alpha_{j1} &= \alpha + i_{j_1} + U_w(\alpha+i_w) + U_f\alpha + U_{oj_{12}}\epsilon_2 + \cdots + U_{oj_{1n}}\epsilon_n \\
\alpha_{j2} &= \alpha + i_{j_2} + U_w(\alpha+i_w) + U_f\alpha + U_{oj_{21}}\epsilon_1 + \cdots + U_{oj_{2n}}\epsilon_n \\
\alpha_{j3} &= \alpha + i_{j_3} + U_w(\alpha+i_w) + U_f\alpha + U_{oj_{31}}\epsilon_1 + \cdots + U_{oj_{3n}}\epsilon_n \\
&\vdots \\
\alpha_{jn} &= \cdots
\end{aligned}$$

for a half wing with n propellers mounted on the leading edge. $U_{oj_{12}}$ presents the upwash effect of the second actuator on the

first one. As long as there is a fuselage between the propellers separating the slipstreams, the upwash effects coming from the other wing can be neglected. Substituting ϵ from (3), results a set of linear equations in the form of $Ax = b$ where, $x = [\epsilon_1, \epsilon_2, \epsilon_3, ...]$

$$A = \begin{bmatrix} -1/E_1 & U_{oj_{12}} & U_{oj_{13}} & \cdots \\ U_{oj_{21}} & -1/E_2 & U_{oj_{23}} & \cdots \\ U_{oj_{31}} & U_{oj_{32}} & -1/E_3 & \cdots \\ \vdots & \vdots & \vdots & \ddots \end{bmatrix}$$

and

$$\begin{aligned} b(1) &= -[\alpha + i_{j1} + U_{w1}(\alpha + i_w) + U_{f1}\alpha] \\ b(2) &= -[\alpha + i_{j2} + U_{w2}(\alpha + i_w) + U_{f2}\alpha] \\ &\vdots \end{aligned}$$

Once the set of linear equations solved, ϵ and therefore the inflow angles α_j can be found.

Similarly, wing inflow angles for sections that are not inside the propeller slipstream will be

$$\alpha_{w_{j1}} = \alpha + i_w + U_f \alpha \tag{11}$$

and for the sections inside the slipstream

$$\alpha_{w_{j\mu}} = \alpha_{w_{j1}} - \epsilon + \sum_{jets} U_{\infty_j} \epsilon \tag{12}$$

where the upwash factor U_{∞_j}, due to other propeller slipstreams, is calculated as if they are infinite falling cylinders, resulting in

$$U_{\infty_j} = 2U_{o_j} \tag{13}$$

2.4 Propeller Normal Force

Once the actuator inflow angles α_j determined, the normal force generated by the propeller can be calculated with the assumption of being proportional to inflow angle.

$$C_N = C_{N_\alpha} \sin \alpha_j \tag{14}$$

where,

$$C_{N_\alpha} = \frac{\mu}{2}\left(1 + \frac{\mu}{2} + \frac{\mu}{1+\mu^2}\right)\frac{4.25\sigma}{1+2\sigma}\sin(\beta + 8) \tag{15}$$

which relies on the solidity σ of the propeller approximated by the blade number N_b and the average blade chord $\bar{c_b}$

$$\sigma = \frac{4N_b}{3\pi}\frac{\bar{c}_b}{b_p} \tag{16}$$

$$\bar{c_b} = 0.16\,(1.25b_{0.25} + 2b_{0.50} + 2b_{0.75} + b_{0.95}) \tag{17}$$

β is the propeller pitch angle measured at 0.75% radius blade location.

2.5 Equivalent Mass Flow Influenced by the Wing

The essential difference between a wing in free stream of speed V_∞, and a stationary wing immersed in a slipstream of the same speed V, is the reduction of the mass flow outside the slipstream and also a reduction in the mass flow influenced by the wing. The wing in free stream is influenced from a mass flow that is passing through a tube surface S_∞ of $\pi b^2/4$ containing the wing tips. However, the wing in a slipstream passing through surface S_j influences a smaller mass flow resulting a reduction in the effective span or aspect ratio of the wing.

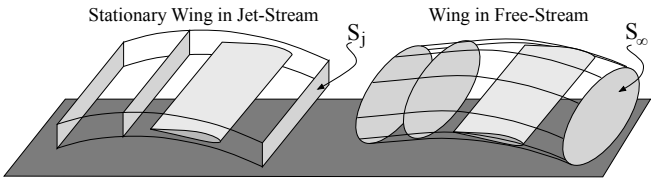

Fig. 6: Mass flow influenced by the wings. On the left: stationary wing in a jet-stream passing through S_j. On the right: wing flying in an equal velocity of free-stream V_∞.

In the case of a stationary wing immersed in a slipstream, compared to a wing in free stream, the same amount of lift has to be generated by deflection of a smaller mass flow through a greater downwash angle. Assuming that the additional downwash angle due to the slipstream is a constant fraction of the downwash of the wing in free stream, with a value of p, then the Aspect Ratio (AR) reduces to

$$AR_0 = \frac{AR}{1+p} \tag{18}$$

2.6 Resulting Lift Slope in a Slipstream

Considering lifting line theory, the lift slope (CL_{α_0}) of this stationary wing in slipstream would be

$$CL_{\alpha_0} = \frac{Cl_{\alpha_{2D}}}{1 + \dfrac{Cl_{\alpha_{2D}}(1+p)}{\pi AR}} \tag{19}$$

where $Cl_{\alpha_{2D}}$ is the lift slope of the two dimensional airfoil.

The calculations relies on the known performance values of the wing in the free stream, so comparing with the lift slope in a free stream which is

$$CL_{\alpha_\infty} = \frac{Cl_{\alpha_{2D}}}{1 + \dfrac{Cl_{\alpha_{2D}}}{\pi AR}} \tag{20}$$

Then, the lift slope CL_{α_0} in static jet slipstream can be calculated by

$$\frac{CL_{\alpha_0}}{CL_{\alpha_\infty}} = \frac{1 + \dfrac{Cl_{\alpha_{2D}}}{\pi AR}}{1 + \dfrac{Cl_{\alpha_{2D}}(1+p)}{\pi AR}} \tag{21}$$

Assuming the two dimensional lift slope value 2π from thin airfoil theory, the ratio function becomes

$$\frac{CL_{\alpha_0}}{CL_{\alpha_\infty}} = \frac{AR+2}{AR+k} \tag{22}$$

where k depends on the slipstream jet aspect ratio.

Jameson[5] has found that a good approximation to the lift of a rectangular wing inside a cylindrical slipstream can be estimated by taking $k = 3.54$. Again, the lift slope CL_{α_∞} of the wing in free stream is assumed to be known.

Similarly, taking into account the forward speed, a wing that is in an elliptic jet slipstream of velocity V_j, with a forward speed of V_∞ will have additional downwash angle compared to the same wing in V_∞ free stream only. This downwash increase is found[10] to be by the factor

$$\frac{\lambda+\mu^2}{1+\lambda\mu^2} \tag{23}$$

where μ is the velocity ratio of V_∞/V_j and λ is the ratio of the width to the height of the slipstream.

This downwash increase results in an equivalent aspect ratio reduction of

$$AR_\mu = AR\,\frac{\lambda+\mu^2}{1+\lambda\mu^2} \tag{24}$$

Using the lift slope of the wing in free stream CL_{α_∞} and stationary within a jet slipstream CL_{α_0}, the characteristics on forward speed can be expressed by

$$\frac{CL_{\alpha_\mu}}{CL_{\alpha_\infty}} = \frac{1}{1+\left(\frac{CL_{\alpha_\infty}}{CL_{\alpha_0}}-1\right)\frac{1-\mu^2}{1+AR_j\mu^2}} \tag{25}$$

where AR_j is the jet slipstream aspect ratio, and will be taken as 1 for circular slipstreams.

2.7 *Partially Immersed Wing in Arbitrary Number of Slipstreams*

The slipstream over the wing will be generated by individual propellers, and also there will be different propulsion configurations for different flight phases, hence an approximation in order to calculate the highly complex force, moments, and interactions. A simple estimation can be made by superposition of forces over the wing in free stream and the individual parts that are immersed in slipstreams. The individual parts that are immersed in slipstream are calculated as isolated planforms. Thus, the additional increase on each isolated planform will simply be the difference between the planform in free stream V_∞, and the planform immersed in a jet slipstream V_j moving with a forward speed of V_∞. The difference in lift will be

$$\Delta L = \frac{1}{2}\rho S_{w_j}(V_j^2\,CL_{\alpha_{j\mu}}\alpha_{w_{j\mu}} - V_\infty^2\,CL_{\alpha_\infty}\alpha_{w_{j_\infty}}) \tag{26}$$

where $CL_{\alpha_{j\mu}}$ is the lift slope of the wing part that is inside the jet slipstream with a velocity ratio of $\mu = V_\infty/V_j$ by taking the aspect ratio as b_j/S_{w_j}. CL_{α_∞} is the lift slope of the same wing part in a freestream, or in other words when $\mu = 1$, $\alpha_{w_{j\mu}}$ is the angle of attack of the wing in jet slipstream, and $\alpha_{w_{j_\infty}}$ is the angle of attack of the same part in free stream. It should be noted that the angle of attack of the wing portion in jet slipstream is reduced compared to the angle of attack in the free stream by the slipstream downwash of ϵ as stated in equation 12.

Additionally, an inclined slipstream to the free stream will generate an external upwash, which can be approximated by assuming the slipstream as a falling cylinder model. The upwash at a distance y from the center axis of the slipstream is $\epsilon b_j^2/2/y^2$

According to [5], the average upwash over the external part of the wing will approximately be $\frac{S_{w_j}}{S}\epsilon$. Taking all upwash effects of propeller jets, the increase in lift can be calculated by multiplying the sum of all slipstream upwash angle with the unblown surface area and the lift slope of the complete wing in freestream CL_{α_∞}

For the small angle of attack, lift force generated by the wing can be found by adding up the freestream lift of the complete wing, the additional lift created from the unblown parts of the wing because of the upwash effects of the jets, and finally the additional lift on the blown sections coming from dynamic pressure increase because of the jet velocities.

$$\begin{aligned} L = {} & 0.5\rho V_\infty^2 S CL_{\alpha_\infty} + \\ & 0.5\rho V_\infty^2 S CL_{\alpha_\infty}\left(S - \sum_{jets} S_{w_j}\right)\sum_{jets}\frac{S_{w_j}}{S}\epsilon + \\ & \sum_{jets}\Delta L_j \end{aligned} \tag{27}$$

2.8 *Induced Drag*

Let k denote CD_i/CL^2, k_{j_0} be the same ratio for a the wing in a static propeller jet slipstream, k_{j_∞} is the wing in a free stream, and k_{j_μ} is the wing in a slipstream with a forward flight velocity ratio of μ. Once again, the induced drag coefficient can be estimated by comparing with the values from freestream, that are assumed known or calculated by lifting-line theory, or empirically. Jameson suggests

$$k = \frac{1+0.006AR}{\pi AR} \tag{28}$$

for the sections inside the jet, the section's $AR_{section}$ will be used. Once the k_{j_∞} calculated by

$$k_{j_\infty} = \frac{1+0.006AR_{section}}{\pi AR_{section}} \tag{29}$$

k_{j_0} and k_{j_μ} for circular slipstream can be found through

$$\frac{k_{j_0}}{k_{j_\infty}} = 1.68 \tag{30}$$

$$\frac{k_{j_\mu}}{k_{j_\infty}} = \frac{1.68 + 0.32\mu^2}{1 + \mu^2} \tag{31}$$

A similar approach can be used to calculate the additional induced drag for the wing section that are inside the slipstream. ΔD_i can be calculated as the freestream lift of this section multiplied by the change in induced downwash angle, plus the new induced downwash angle multiplied by the change in the lift ΔL.

$$\Delta D_i = 0.5\rho V_\infty^2 S_{w_j} CL_{j_\infty}(\alpha_{i_j} - \alpha_{i_\infty}) + \Delta L \alpha_{i_j} \tag{32}$$

where

$$\alpha_{i_\infty} = CL_{j_\infty} k_{j_\infty} \tag{33}$$

$$\alpha_{i_j} = CL_{j_\mu} k_{j_\mu} \tag{34}$$

Note that CL_{j_∞} and CL_{j_μ} were calculated during the ΔL, in (26)

$$CL_{j_\infty} = CL_{\alpha_\infty} \alpha_{w_{j_\infty}} \tag{35}$$

$$CL_{j_\mu} = CL_{\alpha_{j_\mu}} \alpha_{w_{j_\mu}} \tag{36}$$

Finally, induced drag D_i can be found by summing up the induced drag of the whole wing in freestream as if there were no propeller slipstreams on it, and the additional induced drag ΔD_i

$$D_i = 0.5\rho V_\infty^2 S k C L_\infty^2 + \sum_{jets} \Delta D_{i_j} \tag{37}$$

2.9 Viscous Drag

The interest while developing this semi-empirical method is to be able to use it for designing small scale V/STOL UAVs, where the low-Reynolds effects are significantly important and therefore viscous drag addition can not be ignored. Wing in isolation can be solved by a high-fidelity approach in order to have a basis estimate. However this will slow down the solution too much that the whole idea of being fast for rapid development and analysis for conceptual design will be vanished. With this in mind, the same procedure that is used in *QPROP*[11], which is a polynomial fit to the lift-drag curve with an exponential correction coefficient for Reynolds effects is implemented.

2.10 Total Drag

Finally, the total drag force can be found as the sum of D_0 parasitic drag, D_i induced drag, and D_v viscous drag contributions.

$$D = D_0 + D_i + D_v \tag{38}$$

2.11 Rotation of the Section Forces

It should be noted that each wing section inside the propeller slipstream generates a lift force perpendicular to the local flow velocity and the drag force parallel to flow velocity. Therefore they should be rotated back by the propeller slipstream downwash angle ϵ and then summed in order to obtain the total lift force L_∞ and drag force D_∞.

2.12 Effect of Flaps

The effect of flaps are modeled by an increase on the wing angle of attack as presented by Jameson[5]. α/δ_∞ being the flap effectiveness of three dimensional wing in free stream, effective wing incidence angle i_{w_∞} becomes

$$i_{w_\infty} = i_w + \alpha/\delta_\infty \; \delta_e \tag{39}$$

where,

$$\alpha/\delta_\infty = \frac{\sqrt{\alpha/\delta_{2D}} + \alpha/\delta_{2D} \frac{AR+4.5}{AR+2} AR}{\sqrt{\alpha/\delta_{2D}} + \frac{AR+4.5}{AR+2} AR} \tag{40}$$

Likewise for a wing section inside propeller slipstream, effective wing incidence $i_{w_{j_\mu}}$ becomes

$$i_{w_{j_\mu}} = i_w + \alpha/\delta_{j\mu} \; \delta_e \tag{41}$$

and for a circular slipstream,

$$\alpha/\delta_{j\mu} = 1 - \mu^2 + \mu^2 \alpha/\delta_\infty \tag{42}$$

i_{w_∞} and $i_{w_{j_\mu}}$ should be substituted for wing incidence i_w in (7), (11), and (12).

3 Zero Lift Angle of Attack Determination

For cases where the propellers are not aligned with the zero lift angle of attack of the wing, the additional velocity imparted by the propellers will change the zero lift angle of attack of those wing sections. These angles for each section must be found separately. Lift slopes $CL_{\alpha_{j_\infty}}$ and $CL_{\alpha_{j_\mu}}$ can be found by setting $i_w = i_j = 0$ and $\alpha = 1$ in (7), (11), and (12) and calculating up to (27). After recalculating CL_{j_∞} and CL_{j_μ} with $\alpha = 0$, correct wing incidence i_w and actuator incidences i_j, the zero lift angle of attack for each wing section can be found by

$$\alpha_{0_\infty} = \frac{CL_{j_\infty(\alpha=0)}}{CL_{\alpha_{j_\infty}}} \quad and \quad \alpha_{0_j} = \frac{CL_{j_\mu(\alpha=0)}}{CL_{\alpha_{j_\mu}}} \tag{43}$$

4 Wing Lift and Drag at High Incidence

As mentioned before, the propeller slipstreams can significantly reduce the angle of attack of the blown wing sections. This will let the aircraft fly at very large angle of attack during transition and hovering flight phases. The added velocity imparted by the propeller slipstream keeps the flow attached on the blown wing sections where the other sections are already stalled. In such cases, the prediction of forces and moments becomes very difficult. However it is still possible to have a

rough estimate which can give an idea about the performance of the vehicle in these phases.

Maximum lift angle of attack α_{max} is defined for each wing section, and it is assumed that any wing section with a greater inflow angle compared to its maximum lift angle of attack ($\alpha_{w_{j\infty}} - \alpha_{0_j} > \alpha_{max}$), is stalled. In this case, if the stall is on the unblown parts, V_∞ will dominate. Upwash effects are not taken into account as they do not contribute significantly. CL_∞ is thus,

$$CL_\infty = CL_{\alpha_\infty} \tan(\alpha_{max}) \cos(\alpha_{w_{j\infty}} - \alpha_{0_\infty}) \tag{44}$$

For the Stalled sections that are inside the propeller slipstream, the velocity becomes V_j, the inflow angle α_{j_μ} and the lift coefficient becomes CL_{j_μ}. The lift will be calculated without ΔL contribution.

$$CL_{j_\mu} = CL_{\alpha_{j_\mu}} \tan(\alpha_{max}) \cos(\alpha_{w_{j\mu}} - \alpha_{0_j}) \tag{45}$$

Hence, for the drag, stalled wing section lift coefficients (44), (45) and k_{j_∞} , k_{j_μ} coefficients are used.

5 Total Forces and Moments

5.1 Forces

For the moment, only longitudinal flight dynamics is considered, so that the lateral force and moments are assumed to be zero $F_y = M_x = M_z = 0$ as in equilibrium. Contribution of the wing lift L_∞, drag D_∞, propeller thrust T, and propeller normal force N will be taken into account as

$$F_z = L_\infty + \sum_{jets} T \sin(\alpha + i_j) + \sum_{jets} N \cos(\alpha + i_j) \tag{46}$$

$$F_x = D_\infty - \sum_{jets} T \cos(\alpha + i_j) + \sum_{jets} N \sin(\alpha + i_j) \tag{47}$$

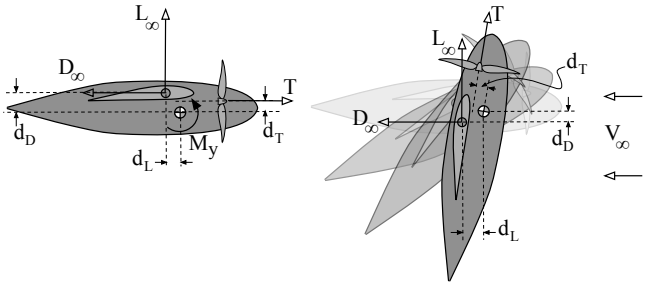

Fig. 7: Illustration of the moment arm length variation during pitch attitude change.

5.2 Moment

The pitching moment is calculated by the resultant wing forces and moments as well. However, as the aircraft is capable of increasing its pitch attitude up to 90 degrees, the moment arm between the wing aerodynamic center and the center of gravity of the aircraft changes during this rotation as shown in Figure 7. The variation on pitch does also effects the position of aerodynamic center of the wing as experimentally tested by Draper and Kuhn [12]. However we will assume it to be fixed. The thrust moment arm d_{T_j} does not change during the pitch variation. However lift force moment arm d_L and drag force moment arm d_D has to be calculated at every angle of attack as a result of moment arm length variation. Finally, the total pitching moment of the aircraft is found by

$$M_y = M_{wing_{AC}} - \sum_{jets} T_j \, d_{T_j} - L_\infty \, d_L + D_\infty \, d_D \tag{48}$$

where,

$$M_{wing_{AC}} = 0.5 \, \rho \, V_\infty^2 \, S_{wing} \, C_M \, \bar{c} \tag{49}$$

$$C_M = \sum_{sections} C_{M_{sec}} \frac{S_{sec}}{S_{wing}} \frac{V_{sec}}{V_\infty} \tag{50}$$

$$C_{M_{sec}} = C_{M_{0_{sec}}} + C_{M_{\alpha_{sec}}} \alpha_{sec} + C_{M_{\delta e.sec}} \delta_{e.sec} \tag{51}$$

6 Equilibrium Calculations

In order to fly in equilibrium at every flight speed (V_∞), the aircraft should sustain

$$F_x = 0 \quad , \quad F_z = 0 \quad , \quad M_y = 0$$

via thrust (T), and elevator deflections (δ_e). For steady cases, this is obtained by finding the roots via a Newton-Raphson iteration. Figure 9 shows the estimated transition angle of attack of the example case aircraft versus horizontal flight speed, where every point is in equilibrium as stated in (6).

7 Preliminary Results

Explained method is parametrized in order to accept multi-variable input, such as the number of propellers, diameter, pitch, position and orientations, wing surface, different thrusts, etc... and written into a FORTRAN code. The final program is capable of analyzing any given configuration within the explained limitations. An example configuration specifications are shown in Table 1.

8 Future Remarks

The propeller slipstreams are taken discrete even though they are really close to each other in some configurations. It could be modified such as that in certain cases with close slipstreams, a rectangular slipstream calculations can be used instead of circular ones as explained in [5].

Wing Span	1.0	$[m]$
Wing Surface Area	0.15	$[m^2]$
Mean Aerodynamic Chord	0.15	$[m]$
Prop Diameter 1/2	0.25/0.15	$[m]$
MTOW (hand-release)	1.8	$[kg]$

Tab. 1: General specifications

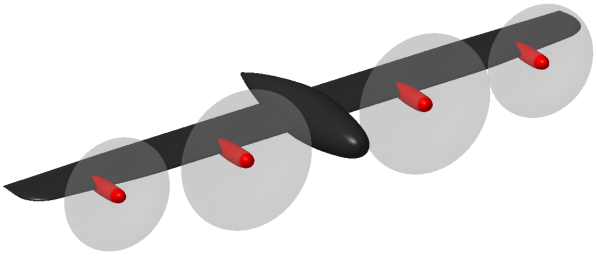

Fig. 8: Representative CAD drawing of the conceptual design.

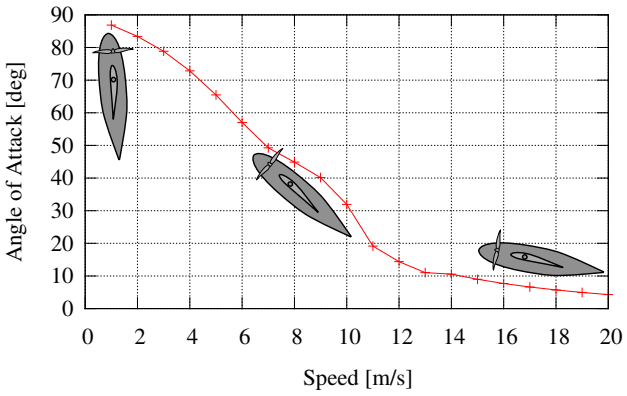

Fig. 9: Estimated variation of angle of attack versus flight speed during equilibrium horizontal transition.

9 Conclusion

A preliminary study on force and moment estimation of a wing with distributed propeller is presented. The method takes into account low-Reynolds effects via airfoil viscous drag contribution. Further verification of the numerical results with wind-tunnel or flight test are required. However, once sufficient confidence is obtained, the method will be useful to design optimized vehicles using this propulsion system configuration, such as the proposed *Next Generation Fixed Wing* aircraft which offers a simplified solution to the wide-speed envelope problem of a fixed wing UAV.

References

[1] Mark D Moore and Bill Fredericks. Misconceptions of electric propulsion aircraft and their emergent aviation markets. In *the 52nd Aerospace Sciences Meeting AIAA SciTech, 17p*, 2014.

[2] Alex M Stoll, JoeBen Bevirt, Mark D Moore, William J Fredericks, and Nicholas K Borer. Drag reduction through distributed electric propulsion. In *Aviation Technology, Integration, and Operations Conference, Atlanta, Georgia*, 16-20 June 2014.

[3] T Ostermann, J Holsten, Y Dobrev, and D Moormann. Control concept of a tiltwing uav during low speed manoeuvring. In *ICAS*, 2012.

[4] Nathan B Knoebel. Adaptive quaternion control for a miniature tailsitter uav, 2007.

[5] Antony Jameson. The Analysis of Propeller Wing Flow Interaction, Analytic Methods in Aircraft Aerodynamics. In *NASA Symposium Proceedings SP-228*, pages 721–749, October 1969.

[6] John De Young. Propellers at High Incidence. *Journal of Aircraft*, 2(3):pp 241–250, May-June 1965.

[7] Richard E Kuhn and John W Draper. An investigation of a wing-propeller configuration employing large-chord plain flaps and large-diameter propellers for low-speed flight and vertical take-off. Technical Report NASA-TN-3307, National Advisory Committee for Aeronautics. Langley Aeronautical Lab., Langley Field, VA, United States, 01 December 1954. ID:19930084052.

[8] S. O. Page V. R. Deckert, W. H. Dickinson. Large-scale wind-tunnel tests of a deflected slipstream stol model with wings of various aspect ratios. Technical Report NASA-TN-D-4448, NASA Ames Research Center, Moffett Field, CA, United States, 01 March 1968. ID:19680009302.

[9] Herbert S Ribner. Notes on the Propeller Slipstream in Relation to Stability. In *NACA ARR L4112a (WRL-25)*, 1944.

[10] C Koning. Influence of the propeller on other parts of the airplane structure. In *Aerodynamic Theory*, pages 361–430. Springer, 1935.

[11] Mark Drela. *QPROP Formulation*. MIT Aero and Astro, June 2006.

[12] John W Draper and Richard E Kuhn. Investigation of the aerodynamic characteristics of a model wing-propeller combination and of the wing and propeller separately at angles of attack up to 90 degrees. Technical Report NACA-TN-3304, National Advisory Committee for Aeronautics. Langley Aeronautical Lab., Langley Field, VA, United States, November 1954. ID:19930092264.